Supplemental Data

Phase-average Method

Evaluating the proper convergence of the mean and statistical parameters is an iterative process. Consequently, we developed a four-phase data processing approach, as illustrated in Figure 1

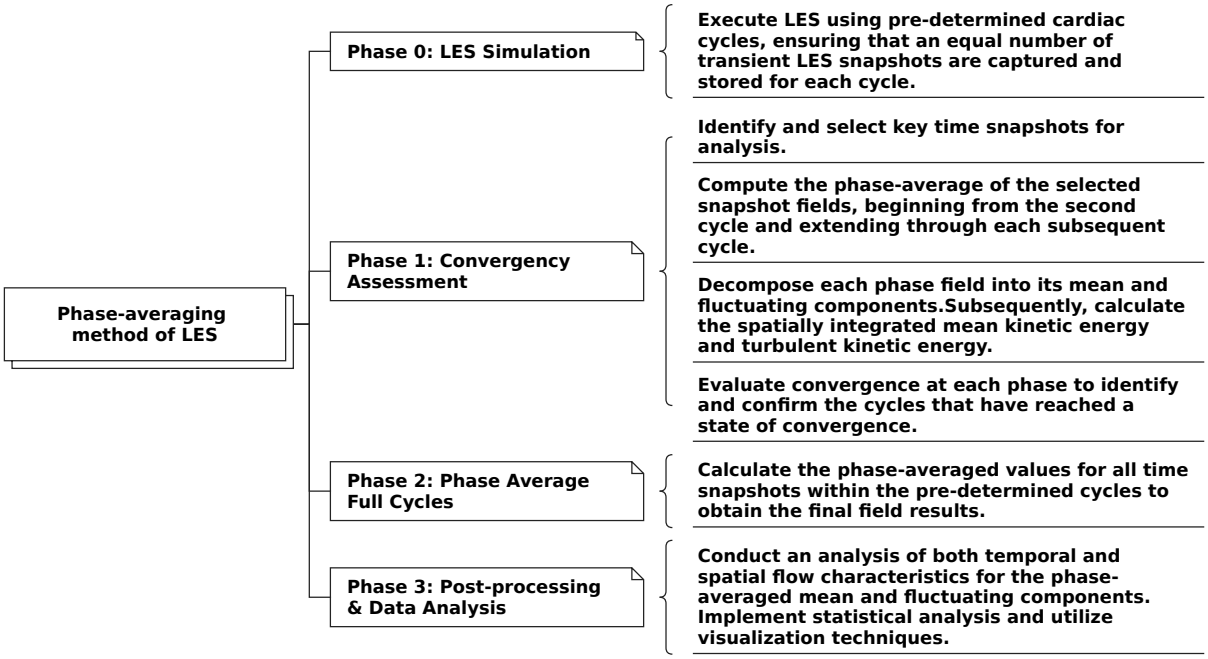

Figure 1. Workflow of Phase-Averaged Method

Numerical Convergence

The second half of the cycles was dedicated to evaluating different cardiovascular parameters in order to ensure that the findings reached accurate statistical convergence. This approach is commonly employed in cardiovascular studies to examine convergence (1; 2). Figure 2 displays the continuous phase-averaged KE and TKE across the aorta during peak systole.

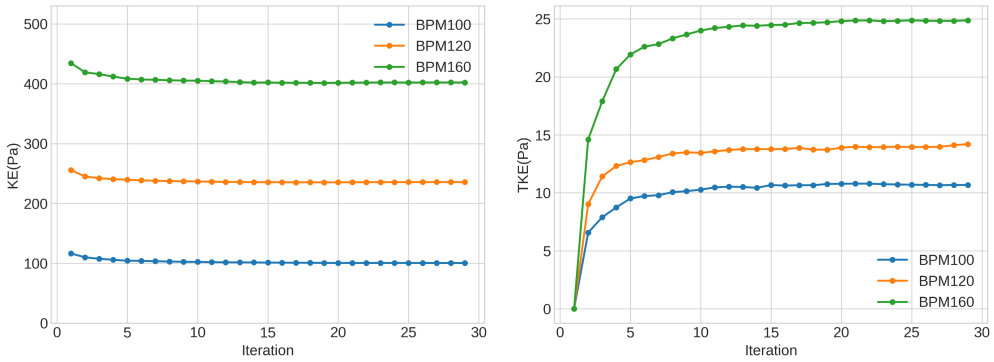

Figure 2. Executing a phase average on the mean KE and TKE, each integrated over the entire aorta at the peak systole activity

Mesh Sensitivity

A total of five unstructured meshes, with cell counts of 2, 4, 6, 8, and 11 million, were generated using the snappyHexMesh tool. Each of the mesh configurations featured five layers of prisms. The final layer was created to have a thickness equivalent to 20% of the size of the cell near the wall, with a growth rate of 1.1. To evaluate the mesh sensitivity, a study was conducted using peak systole flow. The mean velocity was analyzed to assess the impact of the mesh on the variation across different cross sections. The numbers in the analysis correspond to z/D, where D represents the inlet diameter and Z represents the length of the center line geometry depicted in Figure 3. The results of the comparison for the mean velocity in the cross section are illustrated in Figure 4. In this study, a mesh containing 8 million cells was selected, ensuring that the average y plus value remains below 1, covering 99% of the wall surface.

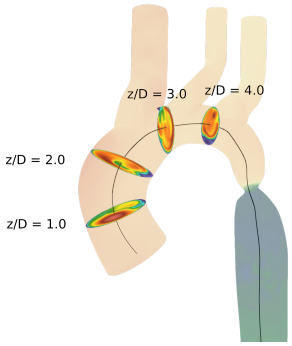

Figure 3. Measurement cross-sections.

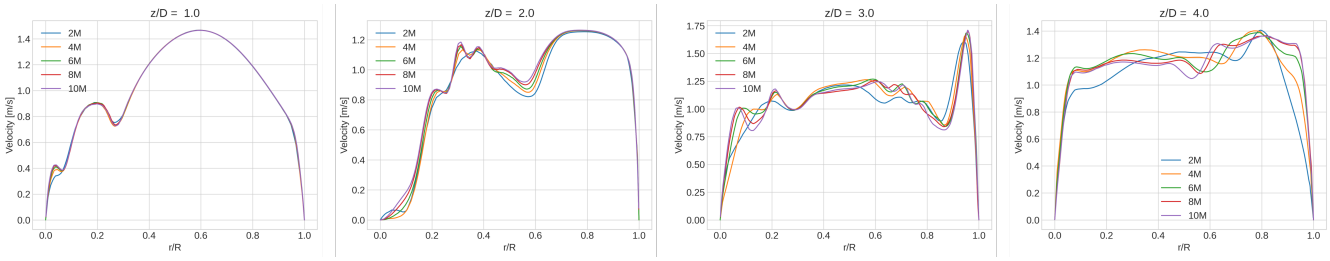

Figure 4. Mean axial velocity at several cross sections with difference mesh size.

Three-element Windkessl Model Coefficient

The Coefficient of 3EWK in the outlet boundary conditions utilized in this study is presented in the table below.

Table 1. Outlet 1 - Brachiocephalic Artery

[h!p]

Coefficient	BPM100	BPM120	BPM160
Z($Pa \cdot s \cdot m^3$)	2.8518e8	2.8518e8	2.8518e8
R($Pa \cdot s \cdot m^3$)	1.2716e9	1.0121e9	6.8781e8
C($m^3 Pa^-1$)	1.2333e-9	1.4800e-9	1.9733e-9

Table 2. Outlet 2 - Left Common Carotid Artery

Coefficient	BPM100	BPM120	BPM160
Z($Pa \cdot s \cdot m^3$)	8.7265e8	8.7265e8	8.7265e8
R($Pa \cdot s \cdot m^3$)	3.2445e9	2.5583e9	1.7005e9
C($m^3 Pa^- 1$)	4.6635e-10	5.5962e-10	7.4615e-10

Table 3. Outlet 3 - Left Subclavian Artery

Coefficient	BPM100	BPM120	BPM160
Z($Pa \cdot s \cdot m^3$)	4.8131e8	4.8131e8	4.8131e8
R($Pa \cdot s \cdot m^3$)	1.9727e9	1.5637e9	1.0525e9
C($m^3 Pa^- 1$)	7.8238e-10	9.8836e-10	1.2518e-9

Table 4. Outlet 4 - Descending aorta

Coefficient	BPM100	BPM120	BPM160
Z($Pa \cdot s \cdot m^3$)	1.9865e8	1.9865e8	1.9865e8
R($Pa \cdot s \cdot m^3$)	1.7905e9	1.4590e9	1.0446e9
C($m^3 Pa^- 1$)	9.6524e-10	1.1583e-9	1.5444e-9

References

1. Lantz, J., Gårdhagen, R. & Karlsson, M. Quantifying turbulent wall shear stress in a subject specific human aorta using large eddy simulation. *Med. engineering & physics* **34**, 1139–1148 (2012).

2. Manchester, E. L. *et al.* Analysis of turbulence effects in a patient-specific aorta with aortic valve stenosis. *Cardiovasc. engineering technology* **12**, 438–453 (2021).